Adsorption-induced anchoring transitions at nematic-liquid-crystal–crystal interfaces

P. Pieranski and B. Jérôme
Laboratoire de Physique des Solides, Bâtiment 510, Faculté des Sciences, Centre Universitaire, 91405 Orsay CEDEX, France

(Received 28 September 1988; revised manuscript received 23 January 1989)

Discontinuous (first-order) anchoring transitions are shown to occur as a function of water adsorption at the nematic-liquid-crystal(*E*9)–gypsum and *E*9-mica interfaces. The transitions involve growth of domains with an anchoring **a'** making a finite angle with the direction **a** of the parent anchoring. The growth proceeds by motion of walls separating the domains with the new anchoring **a'** from the matrix with the parental anchoring **a**. A Landau-type expression for the interfacial energy is proposed and used to classify the anchoring transitions and to explain the behavior of the domains during the first-order anchoring transitions.

I. ANCHORINGS AND ANCHORING TRANSITIONS

The *anchoring* phenomenon, i.e., an orienting action of solid surface on nematic liquid crystals, has been known since the pioneering work by Mauguin[1] and Grandjean.[2] It results from anisotropic interactions of nematic molecules, in the immediate vicinity of the surface, with surface molecules of the substrate on its surface (Fig. 1). The perturbation of the nematic order extends into an interfacial layer of thickness ξ; a surface-induced nematic structure with average local orientation $\mathbf{n}=\mathbf{a}$ results for $z>\xi$. Far from bulk-phase transitions, the thickness ξ, being of the order of magnitude of the correlation length, remains in molecular range and is negligibly small compared to a typical overall thickness of the bulk nematic ($\approx 5\ \mu$m in the present experiments).

The anchoring direction **a**, if it exists, indicates that the energy $F_s(\mathbf{n})$ of the interfacial layer has a minimum for $\mathbf{n}=\mathbf{a}$. For a substrate of symmetry G_s, $F_s(\mathbf{n})$ must be invariant with respect to all symmetry operations $g\in G_s$. Thus, if there is one minimum for $\mathbf{n}=\mathbf{a}$, then identical minima must exist for each of anchoring directions $\mathbf{a}_g=g\mathbf{a}$. The set $\{\mathbf{a}_g\}$ of anchoring directions defines *the type of anchoring.*[3]

One must note that besides possessing the symmetry G_s of the substrate, the energy $F_s(\mathbf{n})$ must also have the usual inversion symmetry of nematics: $\mathbf{n}\equiv-\mathbf{n}$. This means that in the simplest case of *monostable* anchorings the set $\{\mathbf{a}_g\}$ has two equivalent members **a** and $-\mathbf{a}$, while in the case of *bistable* anchoring the set $\{\mathbf{a}_g\}=\{\mathbf{a}_1,-\mathbf{a}_1,\mathbf{a}_2,-\mathbf{a}_2\}$ has four members such that $\mathbf{a}_1\neq\mathbf{a}_2$.

The structure of the interfacial layer and, consequently, its energy $F_s(\mathbf{n})$ as well as the anchoring directions of the set $\{\mathbf{a}_g\}$, can very as a function of different parameters p. Changes in the anchoring directions $\mathbf{a}_g(p)$ can be visualized as trajectories $\mathbf{a}_g(p)$ on a unit sphere representing all possible directions of the anchorings.

The trajectories $\mathbf{a}_g(p)$ can have singularities of two different types: (1) jumps [Fig. 2(a)] and (2) bifurcations [Fig. 2(b)].

The second type of singularities can be considered as a continuous, *second-order anchoring transition.* It has been shown previously that it occurs, for example, as a function of the evaporation angle ϵ, in the case of SiO films evaporated under oblique incidence.[4]

The present paper intends to (i) report observations of discontinuous first-order anchoring transitions occurring at nematic-liquid-crystal–crystal interfaces (Sec. II), and (ii) to build a Landau-type theory upon which a classification of the anchoring transitions can be based, and which can explain several features of the first-order anchoring transitions (Sec. III).

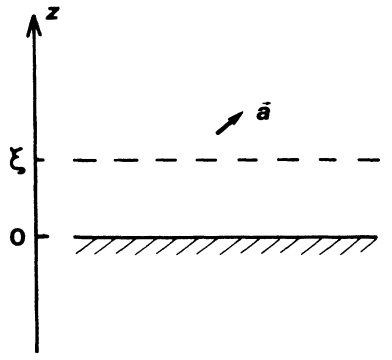

FIG. 1. Definition of the anchoring **a**: the nematic order is perturbed in the interfacial layer of thickness ξ. For $z>\xi$ the perfect nematic order is recovered; its orientation is **a**.

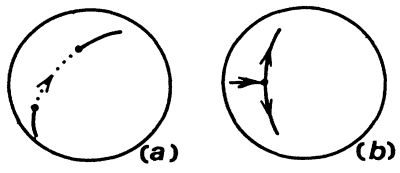

FIG. 2. Changes of the anchorings $\mathbf{a}(p)$ can be represented as trajectories on the unit sphere. The trajectories $\mathbf{a}_g(p)$ can have singularities of two kinds: (a) jumps and (b) bifurcations.

II. EXPERIMENT

A. Cleaved crystal surfaces

As substrates, we have used muscovite mica and gypsum crystals which, because of their layered structures, can be cleaved easily and provide molecularly flat cleavage surfaces. In gypsum[5] [Fig. 3(a)] the (H_2O, $CaSO_4$, H_2O) layers are perpendicular to the [010] direction of the binary axes 2 and 2_1 [Fig. 3(c)] and are separated by the glide planes Σ. As expected from such a structure, cleavage of the gypsum occurs along the glide planes Σ and yields surfaces having C_2 symmetry.

The crystal of muscovite mica[6] can be seen as a stack of alternating layers L_α and L_β [Fig. 3(b)] parallel to the (001) plane and intercalated by potassium ions K. Each of the layers L_α or L_β has a so-called 2:1 structure; *one* Al_2 layer is sandwiched between *two* tetrahedral $(Si_3Al)O_{10}(OH)_2$ layers. In order to provide octahedral cavities for the Al cations of the Al_2 layer, the tetrahedral layers are staggered, one with respect to the other. The layers L_α and L_β differ by the directions of the staggering vectors $\vec{l}_\alpha$ and $\vec{l}_\beta$. These vectors make an angle of 120° and are related each to the other by the symmetry operations of the C_{2h}^6 group. The cleavage of the mica takes place along planes $K_{\alpha\beta}$ or $K_{\beta\alpha}$ [Fig. 3(b)] of the intercalating potassium ions and provides two kinds of symmetryless surfaces related to each other by reflection in the mirror Σ.

B. Experimental setup

Small drops of a nematic-liquid-crystal *E*9 (Ref. 7) were deposited on such surfaces and were allowed to spread (perfect wetting) into a thin layer ($\simeq 5$ μm) (Fig. 4). The samples (S) were then introduced into a cell (C) with glass windows and submitted to a very slow laminar flux i of nitrogen carrying water vapor. The partial pressure p of the water vapor was controlled by mixing two streams i_0 and i_s of, respectively, dry and saturated nitrogen. One has

$$p = p_s \frac{i_s}{i_0 + i_s} , \tag{2.1}$$

where p_s is the pressure of the saturated water vapor.

The observations were made by means of a polarizing

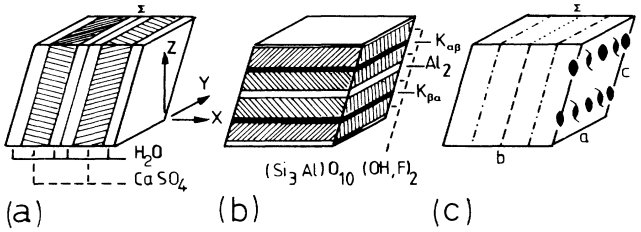

FIG. 3. Schematic representation of the layered structures of (a) gypsum and (b) mica muscovite. Both crystals have the same symmetry C_{2h}^6. Orientations of the glide planes and twofold axes with respect to the crystal layers are visualized in (c).

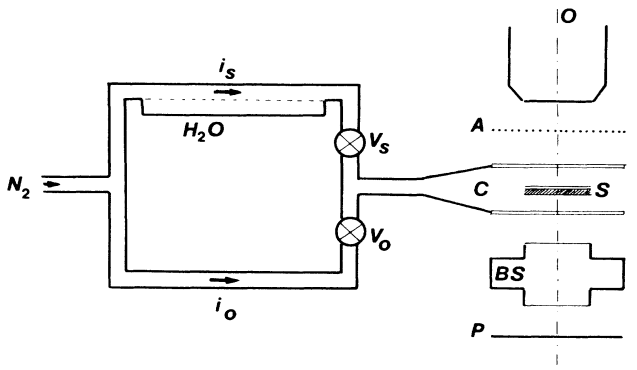

FIG. 4. Experimental setup: s, sample; c, cell; i_0, flux of a dry nitrogen; i_s, flux of nitrogen saturated with water vapor, V_0, V_s valves, B-S compensator.

microscope equipped with a Babinet-Soleil compensator (BS). When properly oriented with respect to the crystal axes of dry mica or gypsum plates, the compensator allows a cancellation of their birefringence. The birefringence of the whole sample (crystal plate plus nematic layer) is then due only to the nematic layer. The anchoring direction **a** can then be determined simply from directions of extinctions of the sample. All experiments were conducted at ambient temperature ($T \approx 20$°C).

C. Results

The results, visualized schematically in Fig. 5, can be summarized as follows.

1. Anchoring directions

We find that the anchoring directions of the nematic *E*9 depend on the water vapor pressure p.

(a) $p < p_c$, "dry anchorings;" on the gypsum surface the anchoring direction **a** makes an angle $\alpha \simeq 90°$ with the [100] axis (fibrous cleavage[8]). On the muscovite mica the direction of the anchoring depends on the type ($K_{\alpha\beta}$ and $K_{\beta\alpha}$) of the cleavage surface. For the $K_{\alpha\beta}$ cleavage surface, the anchoring has a direction $\mathbf{a}_{\alpha\beta}$ which makes an

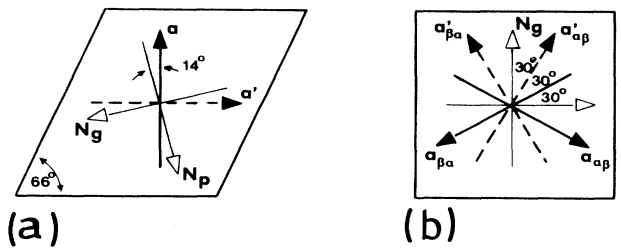

FIG. 5. Schematic representation of the anchorings on surfaces of (a) the gypsum and (b) the mica. **a**, $\mathbf{a}_{\alpha\beta}$, and $\mathbf{a}_{\beta\alpha}$ are the "dry" anchorings ($p < p_c$), while **a**', $\mathbf{a}'_{\alpha\beta}$, and $\mathbf{a}'_{\beta\alpha}$ are the "wet" anchorings ($p > p_c$). The vectors N_g and N_p indicate directions of polarization corresponding, respectively, to the largest and the smallest refractive indices.

angle $\alpha = 60°$ with the [010] axis. In agreement with considerations of Friedel,[8] based on the symmetry C_{2h}^6 of the muscovite mica, the anchoring direction $\mathbf{a}_{\beta\alpha}$ on the cleavage surfaces of the $K_{\beta\alpha}$ type is symmetrical to $\mathbf{a}_{\alpha\beta}$ by reflection in the mirror plane Σ. The anchoring **a** on the gypsum as well as $\mathbf{a}_{\alpha\beta}$ and $\mathbf{a}_{\beta\alpha}$ on the mica are monostable in agreement with symmetries of corresponding surfaces.

(b) $p > p_c$, "moist anchoring;" for larger water vapor pressures, the anchoring direction **a'**, $\mathbf{a}'_{\alpha\beta}$, and $\mathbf{a}'_{\beta\alpha}$ are almost at right angles to, respectively, **a**, $\mathbf{a}_{\alpha\beta}$, and $\mathbf{a}_{\beta\alpha}$. These anchorings are also monostable.

(c) $p = p_c$; the anchoring transitions take place at a critical value p_c of the water vapor pressure. The transition between the "dry" anchoring, for example, **a**, and the "moist" anchoring **a'** is realized, for example, by nucleation and growth of domains with the anchoring **a'** in a matrix (M) with the parent anchoring **a** (Fig. 6). Typical values of the critical relative vapor pressures p_c/p_s are 0.3 and 0.76, respectively, on the muscovite mica and the gypsum.

The above scheme of the anchoring transitions on the muscovite mica and the gypsum emphasizes the similarity of these two transitions involving rotation of the anchoring by $\approx 90°$. However, this scheme is oversimplified as far as the case of the muscovite mica is concerned. In fact, during about half an hour after preparation of a sample on the muscovite mica, not one but three anchoring transitions can be detected. The first transition, occurring at the lowest vapor pressure, is the above one. It is followed, at $p/p_s \approx 0.8$, by a second transition which is also of the first order and which involves a counterclockwise rotation of the anchoring $\mathbf{a}'_{\alpha\beta}$ by 60° into a new direction $\mathbf{a}''_{\alpha\beta}$ [if $\mathbf{a}''_{\alpha\beta}$ was shown in Fig. 5(b) it would be parallel to $\mathbf{a}'_{\beta\alpha}$]. The third transition occurring at $p/p_s \approx 0.95$ rotates the anchoring $\mathbf{a}''_{\alpha\beta}$ clockwise by 60°, which means that the anchoring returns back to the "moist" direction $\mathbf{a}'_{\alpha\beta}$.

After half an hour the second and the third transitions do not occur anymore but the first transition can still be observed for at least several hours. Finally, after several hours, returning from the "moist" anchoring $\mathbf{a}'_{\alpha\beta}$ back to the "dry" anchoring $\mathbf{a}_{\alpha\beta}$ starts to take more and more time (several minutes compared to one second on a fresh preparation) and the anchoring ends to remain in its "moist" direction $\mathbf{a}'_{\alpha\beta}$.

In conclusion, on a scale of 1 h after the preparation of a sample on the muscovite mica, only the first transition, considered in more details here, can be considered as reversible and reproducible. In the case of the gypsum only one transition is observed and it stays reversible and reproducible for days.

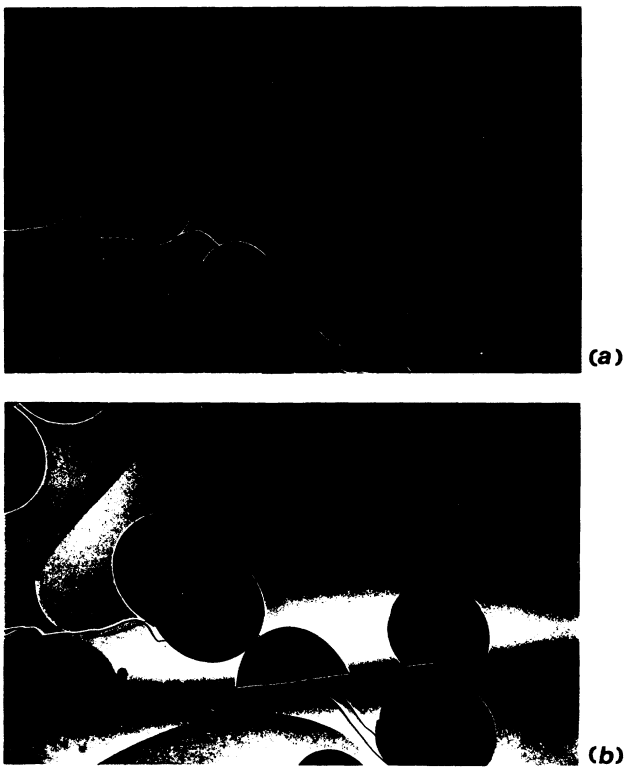

FIG. 6. Photograph of domains with the "moist" anchoring nucleating in a matrix with the "dry" anchoring on the surface of the mica muscovite.

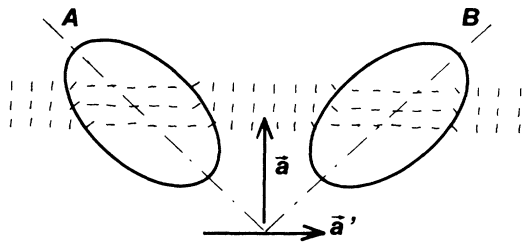

FIG. 7. Two types of domains, A and B, nucleating during the anchoring transition.

2. *Behavior of domains and walls*

On the mica the domains are elliptical in shape and their long axes are directed along bisectrices A or B between the dry, for example, **a** and the moist **a'** anchorings (Fig. 7). Most of the domains nucleating at the anchoring

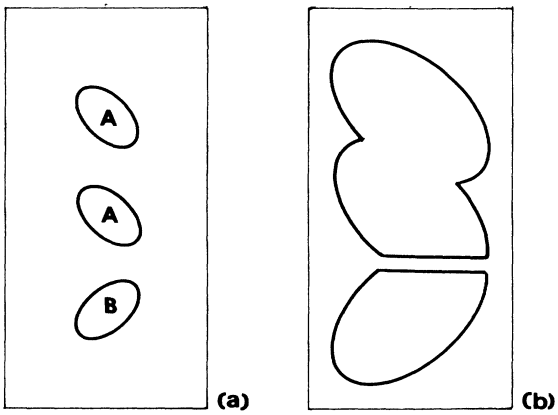

FIG. 8. Evolution of domain walls in the case of adjacent domains of different types.

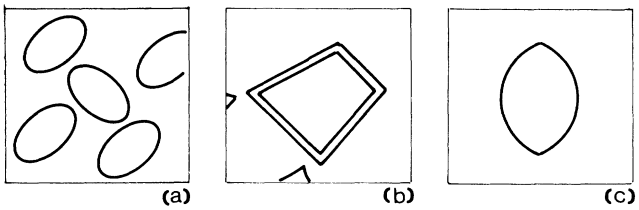

FIG. 9. Transformation of a double wall surrounding a B-type domain into a π disclination for $p > p^+$.

transition are of the same type, for example, A.

When during their growth two adjacent domains touch each other, they coalesce if they are of the same type (A-A or B-B). In the contrary case (A-B) the domain walls preserve their identity, become parallel one to the other, and are separated by a thin band of the parent anchoring (Fig. 8).

When a B-type domain is surrounded by several A-type domains, these last coalesce and a double wall is created around the central B domain. Such a double wall, located at the nematic liquid-crystal–crystal interface transform into a π-disclination loop when the water vapor pressure is increased above a threshold value $p^+ = p_c + \delta p$ (Fig. 9). One has typically on the mica muscovite $p^+/p_s = 0.4$

III. THEORY

A. Interfacial energy

In the framework of a phenomenological Landau-type theory, the existence and evolution of the anchoring directions as well as the behavior of the domain walls (in the case of the first-order transition) have to be interpreted in terms of the interfacial grand canonical potential $\Omega_s = \omega_s A$, where A is the area of the interface (kept constant) and ω_s is the interfacial energy density.[9]

In the present case of an interface between a nematic liquid and a crystal, the interfacial energy not only depends on the partial pressure p_{H_2O} of the water vapor and on the temperature T but also on orientation of the nematic expressed by polar and azimuthal angles (θ,φ). As such, $\omega_s(T,p,\theta,\varphi)$ can be expanded in a series of spherical harmonics:

$$\omega_s(T,p,\theta,\varphi) = \sum_{l,m} Q_{lm}(T,p) Y_l^m(\theta,\varphi) , \tag{3.1}$$

where the amplitudes Q_{lm} are functions of the parameters T and of the vapor pressure p_{H_2O} (the subscript H_2O will be omitted for simplicity).

The general expression (3.1) can be simplified for several reasons. The first important simplification is due to the inversion symmetry of the nematic phase ($\mathbf{n} \equiv -\mathbf{n}$); only terms with even l can be different from zero.

The symmetry G_s of the substrate imposes the next simplifications. For example, in the case of gypsum, $\omega_s(\mathbf{n})$ must be invariant under a rotation C_2, so that all terms with odd m must vanish.

At this stage there are still three $l=2$ and five $l=4$ harmonics. In the vicinity of the anchoring transition all amplitudes $Q_{lm}(T,p)$ vary as functions of the pressure and temperature but only one of them changes sign at the transition. One can then assume that all amplitudes are constant except the one that changes sign under presure variation (the temperature being kept constant).

Finally, by a proper choice of the origin of the azimuthal angle φ one of the $l=2$, $m=\pm 2$ terms can be eliminated. Thus, the second-order contribution to the interfacial free energy writes

$$\omega_s^{(2)}(\theta,\varphi) = Q_{20}(3\cos^2\theta - 1) + \alpha(p - p_c)\sin^2\theta \cos 2\varphi . \tag{3.2}$$

In order to simplify the fourth-order contributions, we assume, in agreement with experimental results, that the minima of $\omega_s(\theta,\varphi)$ are located in the $\theta = \pi/2$ plane (the surface plane). Thus, only the φ dependence of the surface energy has to be considered. The $Q_{4,\pm 2}$ terms have the same φ dependence as the above-mentioned $Q_{2,0}$ and $Q_{2\pm 2}$ terms so that only the $Q_{4,\pm 4}$ terms are pertinent.

The final expression for $\omega_s(\theta,\varphi)$ then takes the form

$$\omega_s(\theta,\varphi) = \omega_s^{(0)}(\theta) + a(\theta)(p - p_c)\cos 2\varphi + c(\theta)\cos 4(\varphi + \psi) , \tag{3.3}$$

where instead of using two amplitudes for the fourth-order term, one amplitude $c(\theta)$ and one phase ψ is introduced.

Knowing that the anchorings are planar, the search for the minima of $\omega_s(\theta,\varphi)$ can be limited to the plane defined by $\theta = \pi/2$. Introducing the notations

$$\begin{aligned} a\left(\frac{\pi}{2}\right) &= a > 0; \quad \left(\frac{da}{d\theta}\right)\Big|_{\theta=\pi/2} = 0 , \\ c\left(\frac{\pi}{2}\right) &= c > 0; \quad \left(\frac{dc}{d\theta}\right)\Big|_{\theta=\pi/2} = 0 , \end{aligned} \tag{3.4}$$

where a and c are constants, one gets

$$\omega_s\left(\frac{\pi}{2},\varphi\right) = \omega_0 + a(p - p_c)\cos 2\varphi + c\cos 4(\varphi + \psi) . \tag{3.5}$$

Using the coefficient c as a natural unit of surface energy, the above expression reduces to

$$\tilde{\omega}_s(\varphi) = \tilde{\omega}_0 + (\tilde{p} - \tilde{p}_c)\cos 2\varphi + \cos 4(\varphi + \psi) , \tag{3.6}$$

where $\tilde{p} = (a/c)p$ is a dimensionless pressure.

B. Discussion

In Fig. 10 are shown three plots of the function $\tilde{\omega}_s(\varphi,\tilde{p})$ for three different values of the parameter ψ. These plots, drawn by computer, can be considered as topographic maps, where a color scale is used to visualize different height levels [values of $\omega_s(\varphi,\tilde{p})$] in the plane $(\varphi,\tilde{p})$. In black and white representation, these plots appear as systems of lines of equal values of ω_s.

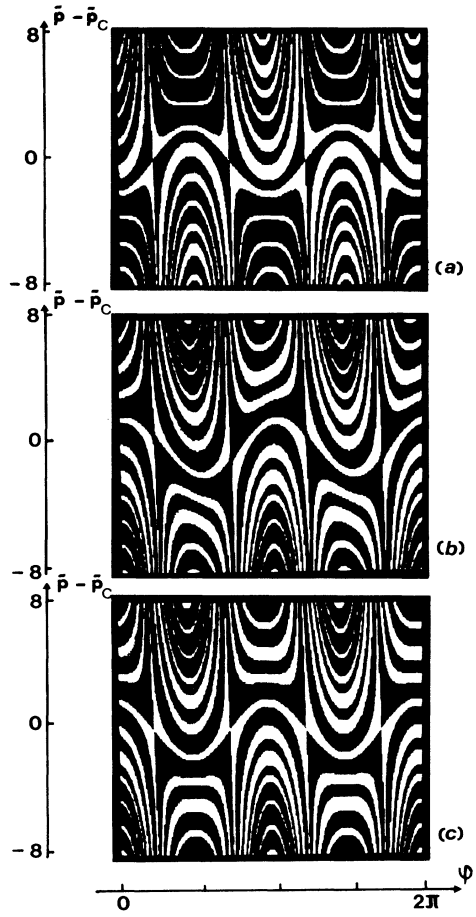

FIG. 10. Plots of the interfacial energy $\tilde{F}_s(\varphi,\tilde{p})$: (a) $\psi=0$; (b) $\psi=\pi/4-0.1$; (c) $\psi=\pi/4$.

1. $\psi=0$: *"Symmetrical" second-order anchoring transition*

For $\tilde{p}<\tilde{p}_-$, there are two valleys, V_0 and V_π located respectively at $\varphi=0$ and $\varphi=\pi$ corresponding to the "dry" anchoring **a** [Fig. 10(a)]. For $\tilde{p}>\tilde{p}_+$, there are also two valleys $V_{\pi/2}$ and $V_{3\pi/2}$ corresponding to the anchoring **a'** ($\perp$**a**). These two systems of valleys are interconnected by bifurcations for intermediate values of the pressure $\tilde{p}$ ($\tilde{p}^- < \tilde{p} < \tilde{p}^+$).

The bifurcations occurring for $\tilde{p}^-$ and $\tilde{p}^+$ correspond to the second-order anchoring transitions which have been discussed in the previous paper.[3]

For $\tilde{p}<\tilde{p}^-$ and $\tilde{p}>\tilde{p}^+$ the anchorings are monostable because the anchoring directions defined by ($\theta=\pi/2$, $\varphi=0$) and ($\theta=\pi/2$, $\varphi=\pi$) as well by ($\theta=\pi/2$, $\varphi=\pi/2$) and ($\theta=\pi/2$, $\varphi=3\pi/2$) are equivalent in each of these pairs.

In the connection region $\tilde{p}^-<\tilde{p}<\tilde{p}^+$, the anchoring is bistable.

2. $\psi=\pi/4$: *"Symmetrical" first-order anchoring transition*

In this case the deepest valleys of the plot are V_0 and V_π for $\tilde{p}<\tilde{p}_c$, and $V_{\pi/2}$ and $V_{3\pi/2}$ for $\tilde{p}>\tilde{p}_c$ [Fig. 10(c)]. As there are no connections between these two sets of valleys, the anchoring transition must be discontinuous. Starting, for example, from the valley V_π at $\tilde{p}<\tilde{p}_c$, the transition can take place either into $V_{\pi/2}$ or into $V_{3\pi/2}$.

As these valleys are of the same depth and are separated from V_π by barriers of the same height, the domains of A-type corresponding to the valley $V_{\pi/2}$ should nucleate with the same probability as the domains of the type B.

When A and B domains are adjacent they are separated by a π wall, where the anchoring direction evolves between $\varphi=\pi/2$ and $\varphi=3\pi/2$. For $\tilde{p}<\tilde{p}^+$ there is a secondary minimum at $\varphi=\pi$. Consequently, the π wall dissociates into two separate $\pi/2$ walls.[10] For $\tilde{p}>\tilde{p}^+$, the π wall can "unstick" from the surface, i.e., transform itself into a bulk π disclination.

3. $0<\psi<\pi/4$: *"Asymmetrical" first-order anchoring transition*

The symmetrical characteristics of the previous two cases are due to the special choice of the phase: $\psi=0$ or $\pi/4$. Such a choice is necessary in the case of a substrate with symmetry C_{2v}. However, in our experiments, the symmetry of the gypsum and mica surfaces were lower. For example, in the case of gypsum the C_2 symmetry allows arbitrary values of the parameter ψ. This, in the most general case, the plot $\tilde{\omega}(\varphi,\tilde{p})$ loses its symmetrical aspect [Fig. 10(b)]. For $0<\psi<\pi/4$ there are bifurcations connecting valleys V_0 and V_π with $V_{\pi/2}$ and $V_{3\pi/2}$, but one of the branches is always deeper then the other. Therefore, the anchoring transition must be first order and takes place at $\tilde{p}=\tilde{p}_c$.

As the nucleation of domains with the new orientation requires some supersaturation, it will occur for a pressure $\tilde{p}=\tilde{p}_c+\delta\tilde{p}$ slightly larger than $\tilde{p}_c$. In such a case the energy barrier separating the valley V_π from $V_{\pi/2}$ is larger than the barrier between V_π and $V_{3\pi/2}$. This fact could explain why nucleation of one type of domains is favored in experiments.

This experimentally observed preference for the nucleation of one type of domain can also be explained by including higher-order terms in the expansion (3.6). For example, in the case of symmetry C_2, $\cos 6\varphi$ and $\sin 6\varphi$ terms can also occur. Due to their presence, the heights of the energy barriers separating the valley V_π from $V_{\pi/2}$ and $V_{3\pi/2}$ would be different even at the transition point $\tilde{p}_c$. In such a case, the discontinuity of the azimuthal angle φ involved in this anchoring transition would be different from $\pi/2$. Finally, if the coefficients of these higher-order terms were also dependent on the vapor pressure $\tilde{p}$, then several anchoring transitions would result from the model for $\tilde{p}$ varying between 0 and 1.

In view of these considerations, the expansion (3.6), is obviously only an approximation which deserves to be seriously improved. However, for the purpose of the present paper, where we are mainly concerned with only one of the anchoring transitions and such that discontinuity of the azimuthal angle is approximately $\pi/2$, the expansion (3.6) with the phase ψ taken different from zero and close to $\pi/4$ seems to be adequate.

IV. CONCLUSIONS

In conclusion, in the present paper we have shown experimentally that first-order, i.e., discontinuous anchoring transitions occur as a function of water-vapor pressure at nematic-liquid-crystal–crystal interfaces. The case of gypsum is very simple as only one reversible and reproducible anchoring transition occurs between $p=0$ and $p=p_s$. Also, a Landau-type theory is particularly simplified for such surfaces with twofold symmetry.

On the other hand, in spite of their susceptibility for a contamination, mica surfaces are very interesting because several anchoring transitions occur for $0<p<p_s$. In the case of muscovite mica we have observed three anchoring transitions. Preliminary observations made with another type of mica (lepidolite) show that a series of three anchoring transitions is also possible. More extensive studies of the anchoring transitions on different types of micas are postponed to another paper.[11]

The work presented in this paper can be extended in several directions.

First of all, evolutions $\mathbf{a}(p)$ of anchorings on other substrates should be tested as a function of several parameters. The most interesting would be crystal surfaces having symmetries different than those of the gypsum and the mica. The pioneering paper by Grandjean[2] provides a very useful starting point as far as the choice of surface is concerned. For a given symmetry, surfaces can differ by their structure so that the number and characteristics of anchoring transitions can vary. In the class of symmetryless surfaces micas offer a very large variety of surfaces due to remarkable polymorphism of these phyllosilicates.

Among the parameters that can affect anchorings, those which are involved in adsorption-desorption mechanisms are particularly interesting. The most obvious and easy to control are vapor pressures of volatile substances. The choice of the water as such an adsorbing substance seems to be crucial presumably because of the capacity of water molecules to form four hydrogen bonds (H_1, H_2, H_3, H_4) at a tetrahedral coordinations. Each water molecule, adsorbed on a surface by two hydrogen bonds (let us say H_1 and H_2) presents the pair of the remaining bonds (H_3, H_4) at right angles to the first pair (H_1, H_2). Thus a layer of water molecules adsorbed on a surface can rotate the anisotropy of the distribution of available hydrogen bonds by $\pi/2$. Such a mechanism could explain the change of sign of the second-order term in the expression (3.2). Our observations of anchoring transition open a number of interesting questions concerning interactions between the molecules of the nematic and the substrate. In particular, the irreversibility observed on the mica substrates should be studied in more detail; chemical reactions occurring at the interface could be at the origin of this irreversibility.

ACKNOWLEDGMENTS

We wish to thank all persons who have offered us samples of minerals: P. Aymard, for gypsum crystals; B. Platevoet, for samples of phyllosilicates; J. Briot; and Société Metafix for samples of micas and vermiculites. We have greatly benefited from discussions with B Platevoet on structures of minerals and with P. Pfeuty and C. Noguera on adsorption phenomena.

---

[1]C. Mauguin, Bull. Soc. Fr. Mineral. Cristallogr. **34**, 71 (1911).

[2]F. Grandjean, Bull. Soc. Fr. Mineral. Cristallogr. **39**, 164 (1916).

[3]B. Jérôme and P. Pieranski, J. Phys. (Paris) **49**, 1601 (1988).

[4]B. Jérôme, P. Pieranski, and M. Boix, Europhys. Lett. **5**, 693 (1988).

[5]W. A. Wooster, Z. Kristallogr. **94**, 375 (1936).

[6]*Micas,* Vol. 13 of *Reviews in Mineralogy,* edited by S. W. Bailey, 2nd printing (Bookcrafters, Chelsea, MI, 1987).

[7]Purchased from British Drug House.

[8]G. Friedel, *Leçons de Cristallographie* (Librairie Scientifique Albert Blanchard, Paris, 1964).

[9]The interface is submitted to exchange of heat and of water molecules with the gas reservoir above the nematic layer. The thermodynamic potential adequate in such a situation is not the free energy F but the grand-canonical potential Ω which is a function of the temperature T and of the chemical potential μ_{H_2O}. T and μ_{H_2O} are the intensive variables characterizing the gas reservoir. The interfacial energy density $\omega_s=\Omega/A$ is therefore a function of these intensive variables. In the perfect gas approximation where μ_{H_2O} is a known function of T and of the partial pressure p_{H_2O} of water vapor, instead of (T,μ_{H_2O}) one can use (T,p_{H_2O}) as variables of ω_s.

[10]F. C. Frank and H. H. van der Merwe, Proc. R. Soc. London, Ser. A **200**, 125 (1949).

[11]P. Pieranski, B. Jérôme, and M. Gabay, in Proceedings of the Conference on Optics and Interfacial Phenomena in Liquid Crystals and Polymers, Torino, 1988 (unpublished).